Hybrid Predictive Control for Tracking in a Single-Phase DC/AC Inverter with an Unknown Load

Haoyue Gao, Mohamed Maghenem, and Ricardo G. Sanfelice

Abstract— **This paper presents a control algorithm for the full H-bridge inverter that renders an arbitrary small neighborhood of a given desired sinusoidal reference trajectory forward invariant. The proposed control algorithm is hybrid and predictive in nature. Moreover, it consists on steering a quadratic Lyapunov function of the tracking errors towards an arbitrarily small value. Hence, the trajectories of the inverter remain sufficiently close to the reference trajectory. The latter is guaranteed in the presence of an unknown resistive load. Indeed, a finite-time estimator is incorporated to the control loop in order to estimate the unknown load in finite time. The simulations illustrating the main result show that the proposed algorithm maintains the frequency of the switches within a reasonable range.**

I. Introduction

The future of energy depends on smart grids that interconnect different power generation sources, such as photovoltaic arrays, wind turbines, hydroelectric generators as well as energy storage units, into a bigger power network. The development of power electronic converters and efficient controllers allows the integration of different types of sources into the smart grid. Inverters are the main technology used to transform a Direct Current (DC) input voltage into a given Alternating Current (AC) output voltage. This can be done by controlling the switching configuration of the inverter. In most cases, DC/AC inverters are controlled using Pulse Width Modulation (PWM) methods [1], [2]. The PWM approach consists in comparing a sinusoidal reference signal to a carrier signal (typically a triangular wave). Then, the change of the switches is triggered whenever the sign of the difference between these two signals changes. There are two main drawbacks to these approaches: the lack of robustness to perturbations due to their open-loop nature and the production of high harmonic distortion [2], [3].

Over the past two decades, advances have been proposed to solve the tracking control problem for DC/AC inverters in a theoretically well-founded manner. Optimization-based approaches that stabilize the solutions towards an invariant set around the reference are used in [4]. Furthermore, in [4] and for a half-bridge DC/AC inverter in the presence of a known load, a control strategy using Linear Quadratic Regulator (LQR) techniques is proposed. This strategy selects the control signal that minimizes the tracking error and guarantees a minimum dwell time between the switching events at the price of not tracking the reference perfectly. More precisely, the error coordinates are shown to converge only to a small neighborhood of the origin. When tracking a general sinusoidal reference, the load can play an adversary role in the tracking-error dynamics. Hence, in [4], the reference trajectory is chosen carefully so that the load plays a positive role. Beside optimal control techniques, some nonlinear control approaches are also present in the literature. For example, a sliding-mode-based control approach is proposed in [5]. However, the performance of this technique is limited due to the chattering phenomenon that inevitably results in slow convergence, low tracking accuracy, and the lack of robustness with respect to disturbances [5]. Also, in [6] and [7], hybrid control algorithms are proposed but in the absence of a load.

In this paper, we extend the hybrid predictive tracking algorithm proposed in [7] by assuming the presence of an unknown resistive load. Indeed, the proposed control strategy consists in selecting the input that forces a quadratic function of the tracking error to decreases, for some time, along the DC/AC solutions. The change of the input is triggered when the quadratic function reaches a given upper bound (tracking precision) and when it is not decreasing along the solutions. The latter generates a hysteresis effect that explains the hybrid nature of the proposed algorithm. Furthermore, when different values for the input can be chosen, we select the one that renders the next triggering time the largest, which explains the predictive nature of the algorithm. Due to the presence of the load, it is not easy to address the tracking problem while considering a general sinusoidal reference. Hence, as in [4], we propose a class of reference signals that allows us to handle the effect of the load. Furthermore, as we assume that the load is unknown, a finite-time hybrid estimator is incorporated in the control loop to estimate the right value of the resistive load in finite time. It is shown, via simulations, that the proposed algorithm delivers a clean AC output voltage, to have a good disturbance rejection ability, and to allow the tracking error to remain within a sufficiently small neighborhood of the origin.

The rest of the paper is organized as follows. Preliminaries on hybrid systems are in Section II. The inverter open-loop model is in Section III. The control problem is formulated in Section IV. The hybrid controller and the finite-time hybrid estimator are introduced in Section V. Finally, the effectiveness of the proposed approach is illustrated via

H. Gao, M. Maghenem, and R. G. Sanfelice are with the Department of Electrical and Computer Engineering, University of California, Santa Cruz. Email: hgao13,mmaghene,ricardo@ucsc.edu.

This research has been partially supported by the National Science Foundation under Grant no. ECS-1710621 and Grant no. CNS-1544396, by the Air Force Office of Scientific Research under Grant no. FA9550-16-1-0015, Grant no. FA9550-19-1-0053, and Grant no. FA9550-19-1-0169, and by CITRIS and the Banatao Institute at the University of California.

simulations in Section VI.

II. Preliminaries on Hybrid Systems

Following [8], a hybrid dynamical system modeled as a hybrid inclusion $\mathcal{H} = (\mathcal{C}, F, \mathcal{D}, G)$ is given by

$$\mathcal{H} : \begin{cases} x \in \mathcal{C} & \dot{x} \in F(x) \\ x \in \mathcal{D} & x^+ \in G(x), \end{cases} \tag{1}$$

where $x \in \mathbb{R}^n$ is the state variable, $\mathcal{C} \subset \mathbb{R}^n$ is the flow set, $\mathcal{D} \subset \mathbb{R}^n$ is the jump set, and $F : \mathbb{R}^n \rightrightarrows \mathbb{R}^n$ and $G : \mathbb{R}^n \rightrightarrows \mathbb{R}^n$ are the flow and jump maps, respectively.

The notion of hybrid arcs is used to define the concept of solutions to $\mathcal{H}$. A hybrid arc ϕ is parametrized by an ordinary time variable $t \in \mathbb{R}_{\geq 0} := (0, \infty)$ and a discrete jump variable $j \in \mathbb{N} := \{0, 1, \dots\}$. Its domain of definition, denoted $\operatorname{dom}\phi$, is a hybrid time domain: it is such that for each $(T, J) \in \operatorname{dom}\phi$, $\operatorname{dom}\phi \cap \big([0,T] \times \{0, 1, \dots, J\}\big) = \cup_{j=0}^{J} \big([t_j, t_{j+1}] \times \{j\}\big)$ for a sequence $\{t_j\}_{j=0}^{J+1}$, such that $t_{j+1} \geq t_j$ and $t_0 = 0$. A hybrid arc ϕ is a solution to $\mathcal{H}$ if it satisfies its dynamics; see [8, Definition 12].

A solution ϕ to $\mathcal{H}$ is said to be maximal if there is no solution ψ to $\mathcal{H}$ such that $\phi(t,j) = \psi(t,j)$ for all $(t,j) \in \operatorname{dom}\phi$ with $\operatorname{dom}\phi$ a proper subset of $\operatorname{dom}\psi$. It is said to be trivial if $\operatorname{dom}\phi$ contains only one element. The system $\mathcal{H}$ is said to be forward complete if the domain of each maximal solution is unbounded. It is said to be pre-forward complete if the domain of each maximal solution is closed. Finally, we use $\mathcal{S}(x_o)$ to denote the set of maximal solutions to $\mathcal{H}$ starting from x_o.

III. The Open-Loop Inverter Model

The circuit diagram of the DC/AC inverter considered in this paper is in Figure 1. The current through the resistor R and the inductor L is denoted by i_L. The current through the capacitor C and the load R_L is denoted by i_C and i_{R_L}, respectively. The output of the H-bridge V_{in} serves as the input voltage for the RLC filter. The H-bridge consists in four single-pole/single-throw (SPST) switches S_1, S_2, S_3, and S_4. Moreover, the switch S_5 defines the connectivity of the resistive load. Each switch is assumed to be ideal and switches instantaneously between "ON" and "OFF". A logic variable $\ell \in \{0, 1\}$ is used to denote the status of S_5; namely, $\ell = 1$ when the switch S_5 is "ON" and $\ell = 0$ otherwise.

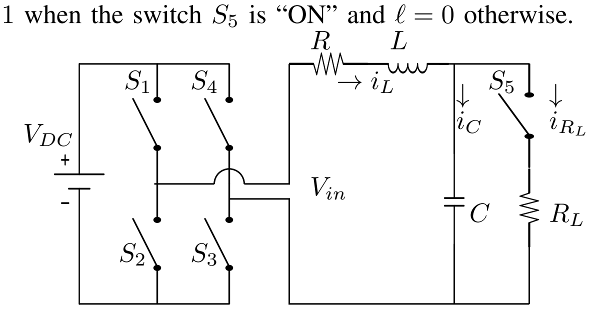

Fig. 1. Single-phase DC/AC inverter with load circuit diagram

Depending on the configuration of the switches, the following three values of the input V_{in} are possible:

$$V_{in} = \begin{cases} V_{DC} & \text{if } S_1 = S_3 = \text{ON and } S_2 = S_4 = \text{OFF} \\ 0 & \text{if } S_2 = S_3 = \text{ON and } S_1 = S_4 = \text{OFF} \\ -V_{DC} & \text{if } S_2 = S_4 = \text{ON and } S_1 = S_3 = \text{OFF}. \end{cases}$$

Applying Kirchhoff's laws to the RLC filter leads to the following three possible dynamics for i_L:

$$\dot{i}_L = \begin{cases} \frac{V_{DC}}{L} - \frac{R}{L} i_L - \frac{1}{L} v_C & \text{if } S_1 = S_3 = \text{ON and } S_2 = S_4 = \text{OFF} \\ -\frac{R}{L} i_L - \frac{1}{L} v_C & \text{if } S_2 = S_3 = \text{ON and } S_1 = S_4 = \text{OFF} \\ -\frac{V_{DC}}{L} - \frac{R}{L} i_L - \frac{1}{L} v_C & \text{if } S_2 = S_4 = \text{ON and } S_1 = S_3 = \text{OFF}. \end{cases} \tag{2}$$

The configuration of the H-bridge affects the dynamics of i_L whereas the connectivity of the switch S_5 impacts the dynamics of v_C as follows:

$$\dot{v}_C = \begin{cases} \frac{1}{C} i_L - \frac{1}{C R_L} v_C & \text{if } S_5 = \text{ON}, \\ \frac{1}{C} i_L & \text{if } S_5 = \text{OFF}. \end{cases} \tag{3}$$

Combining the above, the circuit in Figure 1 is described by the following differential equation with state $z := [i_L \;\; v_C]^\top \in \mathbb{R}^2$ and input $u \in U := \{-1, 0, 1\}$:

$$\dot{z} = \begin{bmatrix} \dot{i}_L \\ \dot{v}_C \end{bmatrix} = f_z(z, u) := \begin{bmatrix} \frac{V_{DC}}{L} u - \frac{R}{L} i_L - \frac{1}{L} v_C \\ \frac{1}{C} i_L - \frac{v_C}{C R_L} \ell \end{bmatrix}. \tag{4}$$

Having $u = 1$ implies that $V_{in} = V_{DC}$, $u = -1$ implies that $V_{in} = -V_{DC}$, $u = 0$ implies that $V_{in} = V_{DC} = 0$. To simplify the presentation, the variable $\ell \in \{0, 1\}$ is treated as a parameter.

IV. Problem Formulation, Reference, and Errors Dynamics

The goal of this paper is to design a controller that solves the following tracking problem.

Problem 1 (Tracking problem): Given a reference signal $t \mapsto z_r(t) := (i_r(t), v_r(t)) \in \mathbb{R}^2$ and a tracking precision $\delta_e > 0$, find $u = \kappa(t, z_r, z) \in U$ such that the tracking error $e := z - z_r$ satisfies

$$|e(t)| \leq \delta_e \quad \forall t \geq 0 \tag{5}$$

without knowledge of R_L. •

The tracking error e is initially small without loss of generality. Indeed, it is always possible to find a controller that, when $|e(t)| > \delta_e$, steers e to $[0, \delta_e]$ in finite time [7].

A. Reference Trajectory Dynamics

The reference voltage v_r is a sinusoidal signal given by

$$v_r(t) := A \sin(\omega t + \theta), \tag{6}$$

where A is its amplitude, ω its frequency, and θ its initial phase angle.

The desired reference current i_r is given by

$$i_r(t) := C\omega A\cos(\omega t+\theta) + \ell A\sin(\omega t+\theta)/R_L. \quad (7)$$

The dynamics of the reference $z_r := [v_r \quad i_r]^\top$ can be computed by differentiating (6) and (7) with respect to time. This leads to

$$\dot{i}_r = -\omega^2 C v_r(1-\ell) + \frac{\ell}{CR_L} i_r - \frac{1+C^2\omega^2 R_L^2}{CR_L^2}\ell v_r$$
$$\dot{v}_r = \frac{1}{C} i_r - \frac{\ell}{CR_L} v_r.$$

Hence, the reference $t \mapsto z_r(t)$ is a solution to the system

$$\begin{bmatrix}\dot{i}_r \\ \dot{v}_r\end{bmatrix} = f_{z_r}(z_r) := \begin{bmatrix} -\omega^2 C v_r + \dfrac{R_L i_r - v_r}{CR_L^2}\ell \\ \dfrac{1}{C} i_r - \dfrac{1}{CR_L} v_r \ell \end{bmatrix}, \quad (8)$$

and with the initial condition

$$\begin{bmatrix} i_r(0) \\ v_r(0)\end{bmatrix} = \begin{bmatrix} C\omega A\cos(\theta) + \frac{A\sin(\theta)}{R_L}\ell \\ A\sin(\theta)\end{bmatrix}. \quad (9)$$

Note that the range of the solution to (8) starting from (9), namely, the set $\{z_r(t) : t \in \operatorname{dom} z_r\}$ is given by the ellipse:

$$\mathcal{Z}_r := \left\{ z_r \in \mathbb{R}^2 : \frac{i_r^2}{(\omega C)^2} + \frac{((\omega C R_L)^2 + \ell)v_r^2}{(\omega C R_L)^2} - \frac{2 v_r i_r}{\omega^2 C^2 R_L}\ell = A^2 \right\}. \quad (10)$$

B. Error Dynamics

The dynamics of $e := [e_i \quad e_v]^\top = z - z_r$ are given by

$$\dot{e} = A_e e + b_e(u, z_r, z), \quad (11)$$

where $A_e := \begin{bmatrix} -\frac{R}{L} & -\omega^2 C \\ \frac{1}{C} & -\frac{1}{CR_L}\ell \end{bmatrix}$, $b_e(u, z_r, z) := [\nu(u, z_r, z) \quad 0]^\top$, and

$$\nu(u, z_r, z) := \frac{V_{DC}}{L}u - \frac{R}{L} i_r + \frac{LC\omega^2 - 1}{L} v_C + \frac{-R_L i_r + v_r}{CR_L^2}\ell. \quad (12)$$

V. A Hybrid Controller for Tracking with an Unknown Load

A. Choice of Quadratic Function of e

To achieve the property in Problem 1, we consider the quadratic function

$$V(e) := e^\top P e, \quad (13)$$

where

$$P := \begin{bmatrix} 1 & \frac{\psi}{2}(1-\ell) \\ \frac{\psi}{2}(1-\ell) & (C\omega)^2 \end{bmatrix} \quad (14)$$

and $\psi := \frac{RC}{L}$. The matrix P is symmetric. Furthermore, for positive constants $C\omega$ and ψ, P is positive definite when $\ell = 1$. However, when $\ell = 0$, P is positive definite if and only if $R < 2\omega L$.

For $\delta > 0$, the $\delta-$sublevel set of V is given by

$$\Lambda(\delta) := \left\{ e \in \mathbb{R}^2 : V(e) \le \delta \right\}. \quad (15)$$

Note that, when P is positive definite, given $\delta_e > 0$, δ can be chosen in the set $(0, \delta_e/\lambda_{min}(P)]$ such that $e \in \Lambda(\delta)$ implies that $|e| \le \delta_e$.

Furthermore, the time derivative of V along the solutions to (4) satisfies the following infinitesimal inequality:

$$\dot{V}(e, u, z_r, z) + \lambda V(e) \le 2e^\top P b_e(u, z_r, z)$$
$$= 2\nu(u, z_r, z)(e_i h + \frac{\psi}{2} e_v(1-\ell)),$$

where $\lambda := 2\ell + (1-\ell)R/L$ is positive (for each $\ell \in \{0,1\}$). Then, V decreases along the solutions to (4) if

$$\nu(u, z_r, z)(e_i h + \frac{\psi}{2} e_v(1-\ell)) \le 0. \quad (16)$$

In turn, (16) holds if the following conditions are satisfied:

$$\begin{cases} \nu(u, z_r, z) > 0 & \text{if } (e_i h + \frac{\psi}{2} e_v(1-\ell)) < 0 \\ \nu(u, z_r, z) < 0 & \text{if } (e_i h + \frac{\psi}{2} e_v(1-\ell)) > 0 \end{cases} \quad (17)$$

B. Admissible Tracking Set

It can be shown that when $z \in \mathbb{R}^2$ is such that

$$\operatorname{sign}\big(\nu(u, z_r, z)\big) = \operatorname{sign}(u) \quad \forall (z_r, u) \in \mathcal{Z}_r \times U, \quad (18)$$

the conditions in (17) can always be enforced by properly choosing u. When $LC\omega^2 \neq 1$, the set of points $z \in \mathbb{R}^2$ for which (18) holds is given by

$$\Gamma := \left\{ z \in \mathbb{R}^2 : |v_C| \le \frac{V_{DC} - RC\omega A}{k} - \ell\frac{AR + \omega AL}{kR_L} \right\},$$

where $k := \left|LC\omega^2 - 1\right|$ and A is as in (6). The set Γ is referred to as the admissible tracking set.

C. Forward Invariance of $\Lambda(\delta)$

Since solving Problem 1 suggests that the set $\Lambda(\delta)$ is to be rendered forward invariant for the closed-loop system, we want to make sure that $e \in \Lambda(\delta)$ and $z_r \in \mathcal{Z}_r$ imply that $z = z_r + e \in \Gamma$. To guarantee this property, the following assumption is imposed.

Assumption 1: Given $\ell \in \{0,1\}$, the positive constants A, L, C, R, ω, R_L, and V_{DC} are such that $LC\omega^2 \neq 1$, $R < 2\omega L$, and there exists $\bar{\delta} > 0$ such that

$$A \le \left(\frac{V_{DC}}{k} - \sqrt{\frac{\bar{\delta}}{(C\omega)^2 - (\frac{RC}{2L})^2(1-\ell)}} \right)\Xi, \quad (19)$$

where $\Xi := k/(k + \omega RC + \frac{R+\omega L}{R_L}\ell)$ and A as in (6). •

Lemma 5.1: Let $\ell \in \{0,1\}$ and let A, L, C, R, ω, R_L, V_{DC}, and $\bar{\delta}$ be positive constants such that Assumption 1 holds. Then,

$$\Lambda(\delta) + \mathcal{Z}_r := \{e + z_r : (e, z_r) \in \Lambda(\delta) \times \mathcal{Z}_r\} \subset \Gamma \quad \forall \delta \in [0, \bar{\delta}].$$

D. Hybrid Control Strategy When the Load is Known

In this section, a hybrid controller is proposed to solve Problem 1 with R_L known. Following [7], the proposed controller $\mathcal{H}_c$ admits $u \in U$ as a state variable and $\eta := (z, z_r) \in \mathbb{R}^2 \times \mathcal{Z}_r$ as input. It is given as

$$\mathcal{H}_c : \begin{cases} \dot{u} = 0 & (u,\eta) \in \mathcal{C}_c \\ u^+ \in G_c(\eta) & (u,\eta) \in \mathcal{D}_c, \end{cases} \tag{20}$$

where $\mathcal{D}_c := \{(u,\eta) \in X : \delta \le V(e) \le \bar{\delta}, \dot{V} \ge -\lambda V(e)\}$, $\mathcal{C}_c := \mathrm{cl}(X \setminus \mathcal{D}_c)$, and $X := U \times \mathbb{R}^2 \times \mathcal{Z}_r$. The map G_c is to define next.

The proposed construction of G_c implements a switching logic that provides an admissible value of u that maintains the error e inside $\Lambda(\delta)$ and, at the same time, maximizes the time between two consecutive updates of u (or jumps). By maximizing the time in between jumps, we reduce the switching frequency, which, in turn, improves the utilization of the switches. The jump map G_c is constructed in three steps:

Step 1 According to (17) and to force V to decrease along the solutions, we define the auxiliary set-valued map

$$\hat{G}_c(\eta) := \{u \in U : (17) \text{ holds}\}.$$

Step 2 If $\hat{G}_c(\eta)$ has more than one element, for each $\hat{u} \in \hat{G}_c(\eta)$ simulate the solution $t \mapsto \hat{\eta}(t)$ to (4) and (8) starting from η along a given time window $[0, T_p]$, where $T_p > 0$ is a parameter of the controller. Then, evaluate the time for the solution to reach the set $\mathcal{D}_c$. This time is denoted as $T_I(\hat{u}, \eta)$ and given by the functional

$$T_I(\hat{u}, \eta) := \inf\{t > 0 : (\hat{u}, \hat{\eta}(t)) \in \mathcal{D}_c\}.$$

Step 3 Using the result in **Step 2**, select the new value of u as the element $\hat{u} \in \hat{G}(\eta)$ that enables the errors to remain within $\Lambda(\delta)$ for the largest amount of time. This mechanism in implemented in G_c as

$$G_c(\eta) := \mathrm{argmax}\{T_I(\hat{u}, \eta) : \hat{u} \in \hat{G}_c(\eta)\}. \tag{21}$$

Proposition 1: Consider the system in (4). Let $\ell \in \{0, 1\}$ and let A, L, C, R, ω, R_L, V_{DC}, and $\bar{\delta}$ be positive constants such that Assumption 1 holds. Then, for each $\delta \in [0, \bar{\delta}]$, Problem 1 is solved by the hybrid controller $\mathcal{H}_c$ in (20). $\square$

The hybrid closed-loop system $\mathcal{H}^o_{cl} = (\mathcal{C}^o_{cl}, F^o_{cl}, \mathcal{D}^o_{cl}, G^o_{cl})$ resulting from (4) and (20) admits as state variable $x^o := (u, z, z_r) \in X$ with the data $G^o_{cl}(x^o) := \big(G_c(z, z_r), z, z_r\big)$ for each $x^o \in \mathcal{D}^o_{cl} := \{(u, z, z_r) \in X : \delta \le V(e) \le \bar{\delta}, \quad \dot{V}(e) \ge -\lambda V(e)\}$, $F^o_{cl}(x^o) := \big(0, f_z(z,u), f_{z_r}(z_r)\big)$ for each $x \in \mathcal{C}^o_{cl} := \mathrm{cl}(X \setminus \mathcal{D}^o_{cl})$, and $G^o_c(z, z_r)$ as defined in (21).

E. Hybrid Finite-Time Estimator of the Load

When the load is unknown, inspired by [9] and [10], we propose a hybrid estimator that estimates the load in finite time. Note that (4) can be rewritten as

$$\dot{z} = f(z,u) + g(z,u)\theta, \tag{22}$$

where $\theta := 1/R_L$ is the parameter to be estimated,

$$f(z,u) := \begin{bmatrix} -\frac{R}{L} & -\frac{1}{L} \\ \frac{1}{C} & 0 \end{bmatrix} z + \begin{bmatrix} \frac{V_{DC}}{L} u \\ 0 \end{bmatrix},$$

and $g(z,u) := [0 \quad -v_C/C]^\top$. Using the construction in [9], the proposed estimator is a hybrid system denoted $\mathcal{H}_e = (\mathcal{C}_e, F_e, \mathcal{D}_e, G_e)$ with state variable $x_e := (\hat{z}, \hat{\theta}_e, w, Q, \eta, \gamma) \in X_e := \mathbb{R}^2 \times \mathbb{R}^2 \times \mathbb{R} \times M\mathbb{B} \times \mathbb{R}_{>0} \times \mathbb{R}^2 \times \mathbb{R}$[1] and input $u_e := (z, u)$, where $\hat{z}$ is the estimate of z, $\hat{\theta}_e$ is the estimate of θ, and w, Q, η, γ are auxiliary state variables. The data of $\mathcal{H}_e$ is given by

$$F_e(x_e) := \begin{bmatrix} f(z,u) + g(z,u)\hat{\theta}_e + k(z - \hat{z}) \\ 0 \\ g(z,u) - w \\ w^\top w \\ -k\eta \\ w^\top(w\hat{\theta}_e + z - \hat{z} - \eta) \end{bmatrix} \tag{23}$$

for each $x_e \in \mathcal{C}_e := \{x_e \in X_e : \det(Q) \le \epsilon\}$, $\epsilon > 0$, where $k > 0$ is a constant, and $G_e(x_e) := \big(z^\top, Q^{-1}\gamma, 0, 0, 0, 0\big)$ for each $x_e \in \mathcal{D}_e := \{x_e \in X_e : \det(Q) \ge \epsilon\}$. The following result is a direct consequence of [9, Theorem 1].

Proposition 2: Consider the system (4) with $\ell = 1$ and L, C, R, A, ω, R_L, and V_{DC} positive constants. Consider an input $t \mapsto u(t) \in U$ and the corresponding solution $t \mapsto z(t)$ starting from a compact set such that, for some $\sigma > 0$ and $\beta > 0$, the following persistency of excitation property holds.

$$\int_{t_o}^{t_o+\sigma} g^\top(z(t), u(t)) g(z(t), u(t)) dt \ge \beta \qquad \forall t_o \ge 0. \tag{24}$$

Then, for k sufficiently large, the solution to $\mathcal{H}_e$ under the input $t \mapsto u_e(t) = (u(t), z(t))$ and starting from each $x_{eo} \in X_e$ is globally bounded. Moreover, $\hat{\theta}_e$ becomes equal to θ right after the second jump. $\square$

F. Closed-Loop System Using the Hybrid Estimator

In this section, we incorporate the hybrid estimator $\mathcal{H}_e$ into the control loop. The estimate $\hat{\theta}_e$ provided by the hybrid estimator $\mathcal{H}_e$ is used by the controller $\mathcal{H}_c$ only once the estimator $\mathcal{H}_e$ achieves the second jump (i.e. once $\hat{\theta}_e$ becomes equal to θ). Before that, the controller $\mathcal{H}_c$ keeps using an internal variable, denoted $\hat{\theta}$, as an estimate of θ. The variable $\hat{\theta}$ remains constant before the estimator $\mathcal{H}_e$ achieves the second jump. However, once estimator achieves the second jump, the variable $\hat{\theta}$ jumps to $\hat{\theta}_e$. To implement this approach, an extra counter variable $\tau \in \{0, 1, 2\}$, initially set to $\tau(0,0) = 0$, is included to track the amount of jumps that the estimator has achieved. Hence, the controller starts using the right value of θ once $\tau = 2$. Indeed, when $\tau = 2$, the controller will know that $\hat{\theta}_e = \theta$ and, thus, $\hat{\theta}$ jumps to $\hat{\theta}_e = \theta$. When $\hat{\theta}$ is equal to θ, z_r becomes a solution to (8) and the control law in (20) is applied. Before the second jump of the estimator, z_r is a solution to (8) while replacing R_L in f_{z_r} therein by $1/\hat{\theta}$. Furthermore, the control input is

[1] $M\mathbb{B}$ is a ball with size of $M > 0$.

computed using the same algorithm in (20) while using $1/\hat{\theta}$ instead of R_L at each step. Combining the estimator $\mathcal{H}_e$ and the controller $\mathcal{H}_c$, the resulting closed-loop system, denoted $\mathcal{H}_{cl}$, admits as state variable $x := (x^o, x_e, \tau, \hat{\theta}) \in X_{cl} := X \times X_e \times \{0,1,2\} \times \mathbb{R}_{\geq 0}$.

Algorithm 1: Closed-Loop hybrid algorithms

Initialization: $\tau(0,0) = 0$.
if $\tau \leq 2$ **then**
  use $\hat{\theta}$ in $\mathcal{H}_c$
else
  $\hat{\theta} = \hat{\theta}_e$
end

Proving that the hybrid closed-loop system $\mathcal{H}_{cl}$ solves Problem 1, consists in showing the two flowing claims:

Cl1. The tracking error e is within the set $\Lambda(\bar{\delta})$ when $\hat{\theta} = \theta$. This might be shown only When $\hat{\theta}$ is initially not very far from θ.

Cl2. Condition (24) is satisfied along the closed-loop solutions $t \mapsto (z(t), u(t))$.

It would be also interesting to show that the resulting closed-loop system $\mathcal{H}_{cl}$ satisfies the hybrid basic conditions, which would guarantee robustness of $\mathcal{H}_{cl}$ with respect to small perturbations [8]. In this paper, we illustrate the latter two claims as well as the robustness of the closed-loop system via simulations. Rigorous proofs are subject to our future work.

VI. Numerical Validation

TABLE I
Simulation parameter

Quantity	Symbol	Value(sim1/sim2)	unit
Input DC voltage	V_{dc}	$220/48$	V
Output amplitude	A	$100/120\sqrt{2}$	V
Output frequency	ω	120π	$rad \cdot s^{-1}$
RLC filter resistor	R	$1/1.5$	Ω
Inductor	L	$2/50$	mH
Capacitor	C	$1.063/0.1407$	mF
Load resistor	R_L	$100/240$	mH
tracking accuracy	δ	$4/2$	

In this section, we present simulation results from two sets of parameters that are used in [7] and [4], denoted by sim1 and sim2, respectively. The system's parameters are in Table I. The simulation run time is $0.5s$ and for the purpose of presentation, we only show $0.02s$ of the simulation result. There are two metrics we use to determine the performance of the algorithm: the amount of switches of the signal u within the simulation run-time and the total harmonic distortion of z for gried-tied inverters whose maximum values are specified in [11]. The total harmonic distortion $t \mapsto X(t)$ measures the quality of the signal and is defined as $THD(X) := \sqrt{\sum_{n=2}^{\infty}(X_n^2)_{rms}}/(X_1)_{rms}$, where X_n is the n^{th} harmonic distortion of the signal X and X_1 is the harmonic distortion at the fundamental frequency. The harmonic distortion and the switching frequency are in Table II. The result in Table II indicates that the controller reduces

TABLE II
Performance of output signal for non-perturbed reference

Quantity	S_5 is OFF sim1/sim2	S_5 is ON sim1/sim2
Amount of switches u	12831/210	12802/162
THD(i_L)	2.1485%/0.6989%	2.2073%/0.9353%
THD(v_C)	1.0311%/0.1821%	1.0479%/0.261%

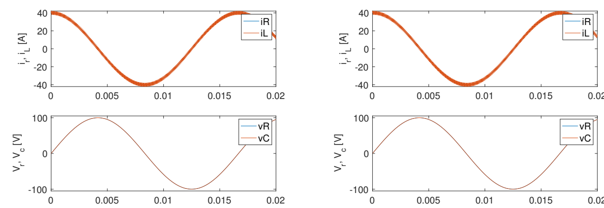

(a) sim1, S_5 OFF (b) sim1, S_5 ON

Fig. 2. Tracking an unperturbed sinusoidal reference for sim1

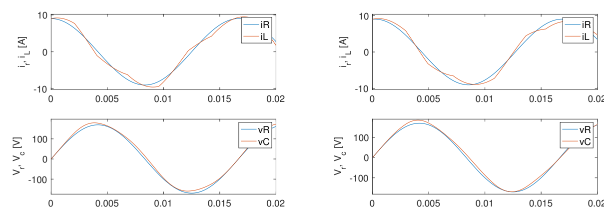

(a) sim2, S_5 OFF (b) sim2, S_5 ON

Fig. 3. Tracking an unperturbed sinusoidal reference for sim2

the amount of switches in the presence of the unknown load at the expense of the THD of the signals. Next, to show robustness of the algorithm, a segmented step noise and a sinusoidal noise are applied to V_{DC}.

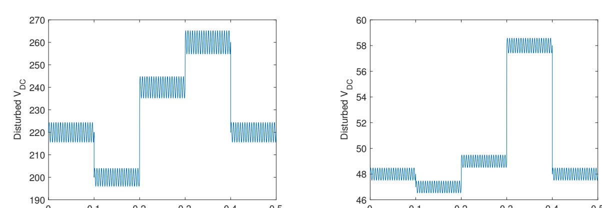

(a) sim1 (b) sim2

Fig. 4. Simulation of the perturbed voltage V_{DC}

The simulations using the parameters in Table I are in Figures 5 and 6. The distortion and the switching frequency are in Table III.

Comparing the results in Tables III and II, we can see

TABLE III

PERFORMANCE OF OUTPUT SIGNAL FOR PERTURBED REFERENCE

Quantity	S_5 is OFF	S_5 is ON
	sim1/sim2	sim1/sim2
Amount of switches u	13356/224	13328/170
THD(i_L)	2.4369%/1.5483%	2.4210%/1.9462%
THD(v_C)	1.0134%/0.3503%	1.0463%/0.6283%

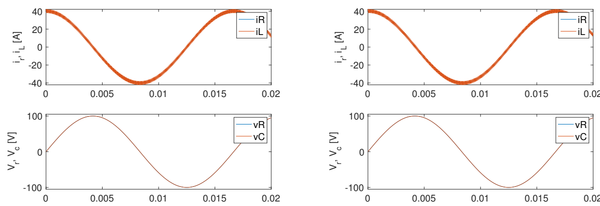

(a) sim1, S_5 OFF (b) sim1, S_5 ON

Fig. 5. Tracking a perturbed sinusoidal reference for sim1

that the switching frequency under a disturbed reference is relatively closed to the one under a non-disturbed reference. Furthermore, the finite-time estimator is illustrated in Figure 7. Figures 8 and 9 show that the errors for converges to a $\Lambda(\delta)$ in finite time. The red dot represents the moment at which the estimator converges to the right value of θ. The corresponding distortion and the switching frequency are in Table IV.

TABLE IV

PERFORMANCE OF OUTPUT SIGNAL FOR ESTIMATOR

Quantity	S_5 is ON	
	sim1	sim2
Amount of switches u	14291	160
THD(i_L)	2.8797%	5.0865%
THD(v_C)	2.5502%	7.8611%

VII. CONCLUSION

This paper presented a hybrid controller for a single-phase DC/AC inverter in the presence and absence of an unknown resistive load. The proposed algorithm guarantees the tracking of a reference signal by showing forward invariance of an arbitrarily small neighborhood around the origin of the tracking errors. Simulations show that the control algorithm is robust to impulsive changes of the reference signal, to small perturbations, and to variations of the DC input voltage, while obtaining harmonic distortion of the output signal within the standard 5% limit, according to [11].

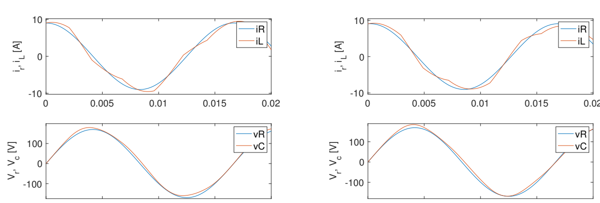

(a) sim2, S_5 OFF (b) sim2, S_5 ON

Fig. 6. Tracking a perturbed sinusoidal reference for sim2

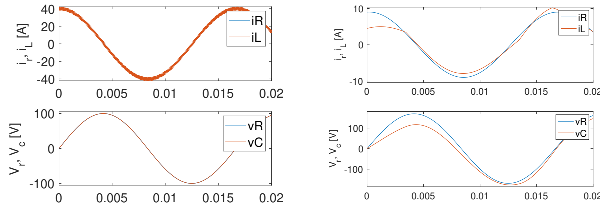

(a) sim1, S_5 ON (b) sim2, S_5 ON

Fig. 7. Tracking the estimated sinusoidal reference

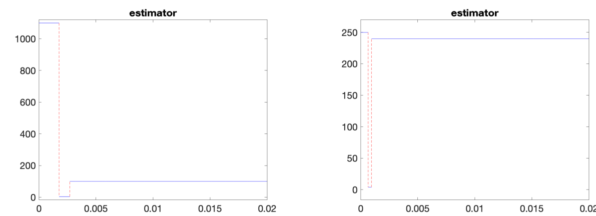

(a) sim1, S_5 ON (b) sim2, S_5 ON

Fig. 8. The parameter $\hat{\theta}$ for the finite-time estimator

REFERENCES

[1] K. Zhang, Y. Kang, J. Xiong, and J. Chen, "Direct repetitive control of SPWM inverter for UPS purpose," *IEEE Transactions on Power Electronics*, vol. 18, no. 3, pp. 784–792, 2003.

[2] J. Holtz, "Pulsewidth modulation for electronic power conversion," *Proceedings of the IEEE*, vol. 82, no. 8, pp. 1194–1214, 1994.

[3] J. Rodriguez, J.-S. Lai, and F. Z. Peng, "Multilevel inverters: a survey of topologies, controls, and applications," *IEEE Transactions on industrial electronics*, vol. 49, no. 4, pp. 724–738, 2002.

[4] C. A. Sanchez, O. L. Santos, D. A. Z. Prada, F. Gordillo, and G. Garcia, "On the practical stability of hybrid control algorithm with minimum dwell time for a DC-AC converter," *IEEE Transactions on Control Systems Technology*, 2018.

[5] H. Komurcugil, "Rotating-sliding-line-based sliding-mode control for single-phase UPS inverters," *IEEE Transactions on Industrial Electronics*, vol. 59, no. 10, pp. 3719–3726, 2011.

[6] J. Chai and R. G. Sanfelice, "A robust hybrid control algorithm for a single-phase DC-AC inverter with variable input voltage," in *Proceedings of the American Control Conference (ACC)*. IEEE, 2014, pp. 1420–1425.

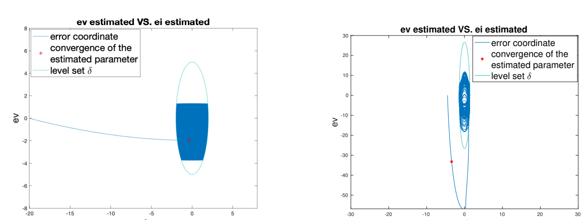

(a) sim1, S_5 ON (b) sim2, S_5 ON

Fig. 9. Phase portrait of the error trajectories

[7] L. Torquati, R. G. Sanfelice, and L. Zaccarian, "A hybrid predictive control algorithm for tracking in a single-phase DC-AC inverter," in *Proceedings of the IEEE Conference on Control Technology and Applications (CCTA)*. IEEE, 2017, pp. 904–909.

[8] R. Goebel, R. G. Sanfelice, and A. R. Teel, *Hybrid Dynamical Systems: Modeling stability, and robustness*. Princeton University Press, Princeton, NJ, 2012.

[9] M. Hartman, N. Bauer, and A. R. Teel, "Robust finite-time parameter estimation using a hybrid systems framework," *IEEE Transactions on Automatic Control*, vol. 57, no. 11, pp. 2956–2962, 2012.

[10] Y. Li and R. G. Sanfelice, "Finite time stability of sets for hybrid dynamical systems," *Automatica*, vol. 100, pp. 200–211, 2019.

[11] IEEE Standards Board, *IEEE Standard for Interconnecting Distributed Resources with Electric Power Systems: 1547-2003*. IEEE, 2003.